Available online at www.sciencedirect.com
SCIENCE DIRECT®
International Journal of Rock Mechanics & Mining Sciences 42 (2005) 531–541
International Journal of Rock Mechanics and Mining Sciences
www.elsevier.com/locate/ijrmms

The joint intersection probability

Y.H. Hatzor[a,*], A. Feintuch[b]

[a]Department of Geological and Environmental Sciences, Ben-Gurion University of the Negev, Beer-Sheva 84105, Israel
[b]Department of Mathematics, Ben-Gurion University of the Negev, Beer-Sheva 84105, Israel

Accepted 4 March 2005
Available online 26 April 2005

Abstract

In this paper a practical method to apply block theory is presented. Block theory provides the removable joint pyramids from a given free surface regardless of the number of joints in any joint intersection. While robust, the application of the theory in real practice is hampered by the large outcome space of possibly removable joint pyramids consisting of k mutually exclusive joints in a rock mass consisting of m joint sets. In this paper, we prove that the probability that k is greater than three in a three-dimensional space is zero. Consequently, only tetrahedral blocks need to be considered in the stability analysis for the analyzed free surface. The outcome space of theoretically removable joint pyramids can be further reduced by considering "safe" joint intersections, which consist of at least one line of intersection which is sub-parallel to the free surface. The block failure likelihood of the remaining joint intersections is proportional to two independent parameters: (1) the joint intersection probability and (2) the block instability parameter. We develop here a rigorous joint intersection probability expression based on simple frequency probability considerations which predicts that the probability for x in the rock mass to fall in joint intersection $L_{i,j,k}$ is inversely proportional to the volume of the parallelepiped formed by joints i,j,k with mean spacing values x_i, x_j, x_k:

$$P(x \in L_{i,j,k}) = \frac{1/V_{i,j,k}}{\sum_{l\neq r\neq s=1}^{m} 1/V_{l,r,s}}.$$

Using the joint intersection probability and the instability parameter associated with each removable JP the critical key blocks of the excavation can be determined. In a brittle rock mass only the critical key blocks will require reinforcement. The paper concludes with a practical example which demonstrates the application of the concepts.

Keywords: Block theory; Geo-statistics; Probability; Rock slope engineering

1. Introduction

1.1. Key block analysis in jointed rock masses

Rock engineering is naturally performed in discontinuous rock masses. Rock discontinuities are typically classified into principal joint sets using statistical procedures. For example, mean orientation may be determined analytically by vector operations or by stereographic projection techniques e.g. [1,2], mean spacing by scan lines surveys in the field e.g. [3,4], and mean trace length by employing convex sampling windows on field exposures e.g. [5,6].

Once the important statistical characteristics of the joint sets (orientation, spacing, and length) are determined with a certain degree of confidence, it becomes essential to predict the type of rock blocks which may form in the rock mass behind the analyzed free surface (rock slope or tunnel face) as a result of joint intersections. The topological key block theory [7] denotes as joint pyramids (JPs) the different half-space combinations that form in the rock mass as a result of joint intersections. For a given free surface block theory

*Corresponding author. Tel.: +972 8 6472621; fax: +972 8 6472997.
E-mail address: hatzor@bgu.ac.il (Y.H. Hatzor).

1365-1609/$ - see front matter © 2005 Elsevier Ltd. All rights reserved.
doi:10.1016/j.ijrmms.2005.03.001

determines the removable JP in the joint intersection using Shi's theorem [7]. Three-dimensional limit equilibrium analysis [8] is then employed by block theory to determine the mechanical stability of the removable JP, provided that the characteristic friction angle for each joint set is known. To perform a comprehensive stability analysis in a jointed rock mass, therefore, one must first characterize the principal joint sets statistically, then find all theoretically removable JPs from the analyzed free surface using block theory, and finally, employ three-dimensional limit equilibrium analysis for each removable JP to determine its failure mode and factor of safety.

1.2. The critical key block concept

Consider now a rock mass with m joint sets. The number of different joint intersections in this rock mass is given by

$$N = \binom{m}{k} = \frac{m!}{k!(m-k)!}, \tag{1}$$

where k is the number of joints which participate in the joint intersection. Note that Eq. (1) is only true for mutually exclusive joints in the intersection. In the simplest case, where each joint intersection produces only one removable JP from the analyzed free surface, the total number of theoretically removable JPs will equal N. This number may be quite large. For example, by applying Eq. (1) to a rock mass consisting of 7 joint sets ($m = 7$), the number of removable JPs of size $k = 3$ is 35, of $k = 4$ is 35, of $k = 5$ is 21, of $k = 6$ is 7, and of $k = 7$ is 1. Hence N in this rock mass equals 99. However, field examinations of block moulds which remained in the excavation surface after the failure of removable key blocks in several engineering case studies [9,10] strongly suggest that only a very limited number of theoretically removable JPs actually materialize in the field as block failures. This field observation implies that not all theoretically removable JPs have the same failure likelihood, namely some JPs are more likely to fail than others.

Hatzor [11] demonstrated, on the basis of many case studies, that the block failure likelihood ($P(B)$) is proportional to two mutually independent parameters:

(1) The joint combination probability (P(JC)) which depends on the spacing and orientation of the joints in the intersection.

(2) The JP instability parameter (F) which maps the required support force for limit equilibrium (F^*) normalized by the active resultant (R) to a field between 0 and 1 for infinitely stable and falling blocks, respectively.

The mathematical expressions for P(JC) and (F) can be found in [11]. The product

$$P(B) = P(\mathrm{JC})(F) \tag{2}$$

provides the block failure likelihood for each JP in the outcome space of Eq. (1) above.

By comparing the resulting $P(B)$ values for all theoretically removable JPs from a given free surface one can readily assess the JPs which are more likely to fail, originally referred to as Critical Key Blocks by Hatzor and Goodman [10]. Previous field studies of both underground openings and rock slopes [9–12] have indicated a very good agreement between predicted $P(B)$ values and mapped block moulds on excavation faces, all of which represented the theoretically determined critical key blocks.

1.3. Safe and unsafe joint intersections

A joint intersection L_{ijk} may yield a removable JP from an analyzed free surface with high failure likelihood and yet may not produce actual block failures in the field. Such joint intersections were referred to as Safe Joint Combinations by Hatzor [9]. Safe joint intersections occur when a line of intersection I_{ij} between two joints in L_{ijk} is sub-parallel to the analyzed free surface. A safe joint intersection may easily be detected using the stereographic projection because in such a case one line of intersection will plot very near the free surface.

Recall that by Shi's theorem [7], a removable JP must plot entirely within the space pyramid (SP): JP $\subset$ SP, or equivalently, the intersection of a removable JP with the excavation pyramid (EP) is empty: JP $\cap$ EP $= \emptyset$. By means of stereographic projection, the implication of Shi's theorem is that all lines of intersections I_{ij} in a removable JP must plot completely within the region of the space pyramid.

In Fig. 1 (A–D) four different joint intersections are plotted and in each case the theoretically removable JP from the analyzed free surface (dashed line), is clearly marked. Note that joint intersections 1 and 4 (Figs. 1A,D) are "safe" because the line of intersection $I_{2,3}$ plots very near the free surface. Therefore, while JPs 110 and 101 in joint intersections 1 and 4 are theoretically removable, any slight deviation in the joint or free surface attitude may shift $I_{2,3}$ into the excavation pyramid, thus producing a non-removable block. Furthermore, if the block does materialize in the field, it will have a very slender shape because of the sub-parallelism between $I_{2,3}$ and the analyzed free surface, as shown in the three-dimensional diagrams on the right in Figs. 1A and D. Such slender blocks will pose minimal risk to the excavation and should not be of great concern.

It is therefore necessary to check the outcome space of Eq. (1) for "safe" joint intersections, namely for any

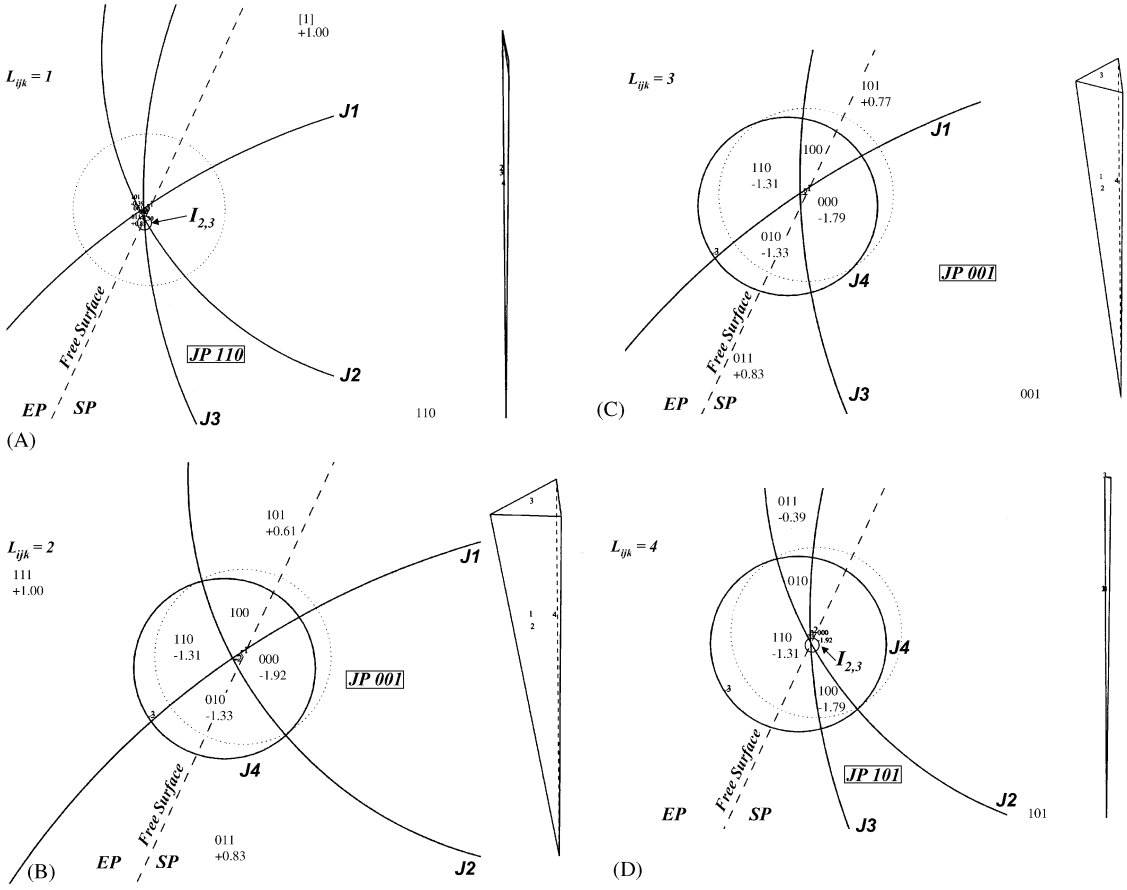

Fig. 1. Left: block theory removability analysis for the four joint intersections listed in Table 2 (Upper hemisphere stereographic projection). The free surface is dashed. Right: removable block geometry. Viewer is looking horizontally along the strike of the free surface towards NE.

joint intersection L_{ijk} that contains a line of intersection I_{ij} which is sub-parallel to the analyzed free surface. The detected "safe" intersections may be eliminated from any further treatment and thus the theoretical outcome space of removable JPs is further reduced.

1.4. Scope of this paper

In this paper we first present a proof that in a jointed rock mass consisting of m joint sets the probability of finding a joint intersection consisting of more than three joints is zero. To appreciate the significance of this proof note that by employing it the outcome space of Eq. (1) reduces from 99 to 35 theoretically removable JPs which must be analyzed in a particular free surface excavated in a rock mass with seven joint sets. This proof explains earlier field observations which indicated that tetrahedral blocks ($k = 3$) were by far the most common underground [9–11]. Furthermore, it lends support to previous analytical attempts to determine the joint intersection probability for the case of tetrahedral blocks only [13]. We then proceed to develop a rigorous joint intersection probability expression, starting in two dimensions and then generalizing to three dimensions using simple frequency probability considerations. Finally, a practical application is provided for the benefit of practitioners.

In developing our solutions we make two assumptions:

(1) all fractures in a joint set are strictly parallel,
(2) all fractures within a given joint set have non-zero spacing.

In nature fracture attitudes within a given joint set exhibit dispersion about a resultant which may be described for example by means of the Fisher constant for normal distributions [14]. Nevertheless, removability and stability analyses in rock mechanics typically assume a fixed orientation for each joint set. Our approach is not different in that sense. Solving the joint intersection probability for a distribution of orientations about each mean attitude is beyond the scope of this paper and is not attempted here.

We also assume that fractures within a joint set have non-zero spacing, namely the spacing cannot be smaller than some threshold value. This assumption is valid for all practical applications in rock mechanics.

2. Line intersections

We begin with some preliminary remarks about the probability of geometric events in the plane. We consider a simple example. Suppose $C = \{(x, y) : x^2 + y^2 = 1/\pi\}$. C is of course the disk of radius $1/\sqrt{\pi}$ with area 1. We look at C as a target and want to consider the probability of hitting a sub-set of C.

A standard model is obtained by considering a probability function which is defined axiomatically on sets for which we have a notion of area, and the probability of hitting such a subset is its area. In this framework points are assumed to have area zero and thus the probability of hitting a given point is zero. This does not mean that there is no possibility of ever hitting a particular point. It simply means that in the standard geometric probability framework hitting a particular point is a non-generic event. In addition, it follows from the standard axioms for probability functions that the probability of hitting one of a sequence of points (a *countable* set) is also zero.

Our statements about the probability for line intersections on a plane and for joint intersections in three dimensions are to be understood in this sense. The mathematical probability of an event taking place should not be identified with the physical possibility of such an event. The notions are closely related but not identical [15].

Before we attempt to solve the three-dimensional problem pertaining to the intersection probability of joint sets within a given rock mass volume, it is instructive to first consider the two-dimensional case pertaining to the intersection of lines on a plane.

In this section we assume that lines are perfectly planar, and that the line spacing in each family is constant, but not necessarily equal. The main point is that by choosing an appropriate algebraic basis for the plane (2-dimensional Euclidian space R^2) we can represent the intersection points of two families of parallel equidistant lines as the set of pairs of integers $\{(n, m)\}$.

2.1. The probability for line intersections on a plane consisting of more than two lines is zero

Consider two families of parallel equidistant lines:

$$F_1: \quad a_1x + b_1y = nc_1,$$
$$F_2: \quad a_2x + b_2y = nc_2, \tag{3}$$

where n varies over the integers. Assume that we have already normalized so that the origin is an intersection point of lines from each family ($n = 0$). Let us now characterize the points of the "grid" determined by the intersection points (Fig. 2).

A point of intersection is a solution of the system of equations:

$$a_1x + b_1y = nc_1,$$
$$a_2x + b_2y = mc_2. \tag{4}$$

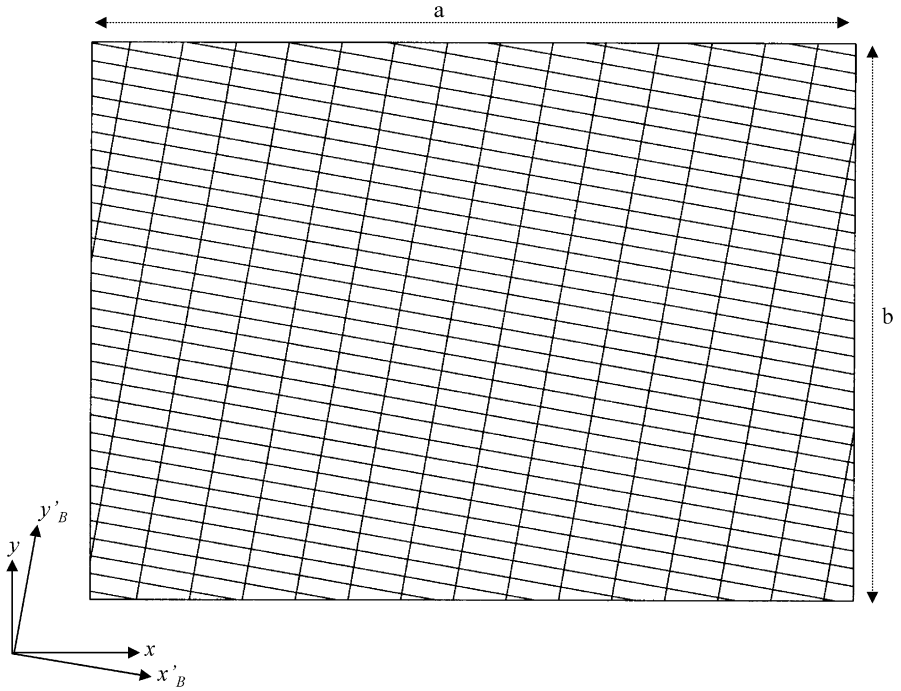

Fig. 2. Trace lines of two joint sets on a plane dipping 90° (vertical) to azimuth 135°. Joint plane dips are as follows: $J_1 = 10/045$; $J_2 = 80/225$. Mean joint spacing values are: $x_1 = 1$ m, $x_2 = 3$ m. Width a and Height b of domain are $a = 44$ m, $b = 32$ m.

Then the x value of the intersection is given by

$$x = \frac{\begin{vmatrix} nc_1 & b_1 \\ mc_2 & b_2 \end{vmatrix}}{\begin{vmatrix} a_1 & b_1 \\ a_2 & b_2 \end{vmatrix}} = nl_1 + ml_2, \tag{5}$$

where l_1, l_2 are easily computed but not important as they depend on a_i, b_i, and c_i. The y value is given by

$$y = \frac{\begin{vmatrix} nc_1 & a_1 \\ mc_2 & a_2 \end{vmatrix}}{\begin{vmatrix} a_1 & b_1 \\ a_2 & b_2 \end{vmatrix}} = ns_1 + ms_2, \tag{6}$$

where s_i, m_i are easily computed as above. Let

$$e_1 = \begin{bmatrix} l_1 \\ s_1 \end{bmatrix}, \quad e_2 = \begin{bmatrix} l_2 \\ s_2 \end{bmatrix}.$$

Then each intersection point is of the form

$$\begin{bmatrix} x \\ y \end{bmatrix} = ne_1 + me_2. \tag{7}$$

Since $B = \{e_1, e_2\}$ is a basis for R^2, we can characterize the grid points as the set of all pairs of integers $\{n, m$ integers$\}$ where (n, m) is the co-ordinate vector of the point with respect to B:

$$\begin{bmatrix} x \\ y \end{bmatrix}_B = \begin{bmatrix} n \\ m \end{bmatrix}. \tag{8}$$

We want to discuss the probability of an arbitrary line intersecting the points of our grid. This of course will depend on the probability function that we define on the appropriate family of subsets, the "measurable" sets. We will follow the tradition that axiomatically associates with each finite line segment in the plane a probability directly proportional to its length (or with a finite plane in R^3 a probability directly proportional to its area). For such a probability measure it is immediate that points have probability zero.

We now refer to the standard sigma—algebra property of probability measures: If T_1, T_2, ... is a sequence of measurable sets which are point-wise disjoint ($T_i \cap T_j = \emptyset$, $i \neq j$) and $T = \cup_{i=1}^{\infty} T_i$, then the probability measure of T, $P(T)$ is just the infinite sum $\sum_{i=1}^{\infty} P(T_i)$. Applying this to our grid we obtain that the probability measure of the set of pairs $\{(n, m)\}$ of integers in the plane is zero. Thus this will be the probability of its intersection with any line. This argument generalizes in an obvious way to the three-dimensional case.

It is easy to extend these arguments to the situations where the spacing between the parallel lines in each family is not uniform as long as it is bounded from below.

3. Joint intersections

The theory developed above for two dimensions is expanded here for three dimensions to address joint intersections within the volume of a rock mass, where the intersection of planes in space replaces line intersections on a plane.

3.1. The probability for a joint intersection consisting of more than three joints is zero

Here everything is the same as in Section 2.1. We consider three families of parallel equidistant planes analogous to three joint sets each of which has a constant spacing value:

$$\begin{aligned} F_1: &\quad a_1x + b_1y + c_1z = nd_1, \\ F_2: &\quad a_2x + b_2y + c_2z = nd_2, \\ F_3: &\quad a_3x + b_3y + c_3z = nd_3, \end{aligned} \tag{9}$$

where again we have normalized and assumed that the origin is a point of intersection of representatives of the families ($n = 0$).

A point of intersection of representatives of each family is a solution to the system

$$\begin{aligned} a_1x + b_1y + c_1z &= nd_1, \\ a_2x + b_2y + c_2z &= md_2, \\ a_3x + b_3y + c_3z &= kd_3. \end{aligned} \tag{10}$$

Here

$$x = \frac{\begin{vmatrix} nd_1 & b_1 & c_1 \\ md_2 & b_2 & c_2 \\ kd_3 & b_3 & c_3 \end{vmatrix}}{\begin{vmatrix} a_1 & b_1 & c_1 \\ a_2 & b_2 & c_2 \\ a_3 & b_3 & c_3 \end{vmatrix}} = nr_1 + mr_2 + kr_3 \tag{11}$$

and similarly

$$\begin{aligned} y &= ns_1 + ms_2 + ks_2, \\ z &= nt_1 + mt_2 + kt_3. \end{aligned} \tag{12}$$

Then

$$\begin{bmatrix} x \\ y \\ z \end{bmatrix} = ne_1 + me_2 + ke_3, \tag{13}$$

where

$$e_1 = \begin{bmatrix} r_1 \\ s_1 \\ t_1 \end{bmatrix}, \quad e_2 = \begin{bmatrix} r_2 \\ s_2 \\ t_2 \end{bmatrix}, \quad e_3 = \begin{bmatrix} r_3 \\ s_3 \\ t_3 \end{bmatrix}$$

form a basis B for R^3. Then

$$\begin{bmatrix} x \\ y \\ z \end{bmatrix}_B = \begin{bmatrix} n \\ m \\ k \end{bmatrix} \tag{14}$$

and again, this set has probability measure zero so the probability of an arbitrary plane passing through such a set is zero.

4. The relative probability of joint intersections

A model for relative probabilities of joint intersections was considered by Mauldon [13]. We present here a different model based on simple frequency probability considerations. Following Mauldon we discuss the model in the case of points of intersections of lines in a plane, and then the straightforward generalization to the three-dimensional case.

Suppose there are m sets Λ_i, $i = 1, \ldots, m$ of parallel lines in the plane. To simplify matters we assume that in each family the distance between any two lines (the spacing) is constant. This assumption is for convenience only. As long as the sequence of distances is bounded below, the following argument is applicable.

If we define $L_{i,j} = \Lambda_i \cap \Lambda_j$, $i \neq j$, the set of intersection points of lines from the families Λ_i and Λ_j, then by Eq. (1) there are $\binom{m}{2}$ such sets. On the basis of the results of the previous sections it is natural to assume that these sets have no common points. Thus our sample space is $L = \cup_{i \neq j=1}^{m} L_{i,j}$, where $L_{i,j} \cap L_{k,l} = \emptyset$ for $i \neq k$ or $j \neq l$.

We want to define a probability function on this sample space which is appropriate to answer the question: "What is the probability that $x \in L$ belongs to a given $L_{i,j}$"?

The sets $L_{i,j}$ are infinite sets. However, if we choose a large circle with center at the origin of radius R, then we can give a good simple approximation of the number of points of $L_{i,j}$ inside this circle. If we identify each point with the lower left vertex of the parallelogram determined by the intersections of the families of lines Λ_i and Λ_j, then there are two types of points in the circle. The first type is those points whose associated parallelogram is completely in the circle, and the second type is those whose associated parallelograms contain a part of the circumference of the circle (Fig. 3). It is not hard to see

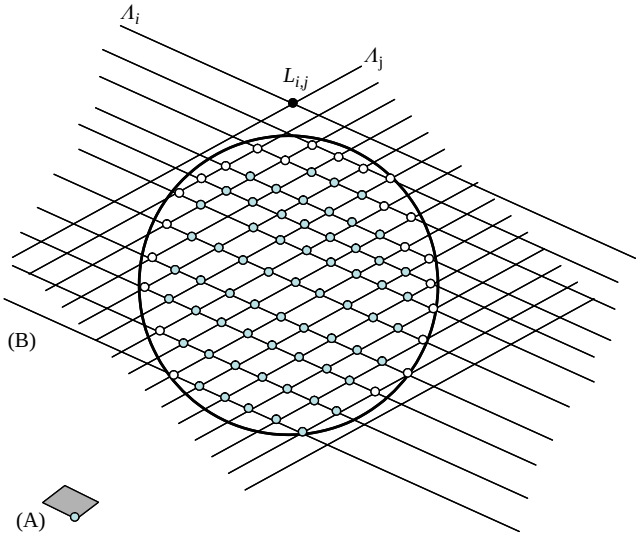

Fig. 3. (A) A point in the grid and its associated parallelogram of area a, (B) schematic presentation of the two types of points in a sampling circle of radius R: filled points—associated parallelograms are completely contained in the circle; open points—associated parallelograms contain a part of the circumference of the circle.

that for R sufficiently large, the number of points of the second type becomes negligible relative to the number of points of the first type.

If a_{ij} denotes the area of the parallelograms determined by Λ_i and Λ_j, then $\pi R^2/a_{i,j}$ is thus a good approximation for the number of intersection points inside the circle (This can be made precise but the details are not important in this context.). Thus, a good approximation for the number of points of L in the given circle is $\sum_{k \neq j=1}^{m} \pi R^2/a_{k,l}$ and the frequency probability that a given point x in m belongs to L_{ij} is given by

$$\frac{\pi R^2/a_{i,j}}{\sum_{k \neq j=1}^{m} \pi R^2/a_{k,j}} = \frac{1/a_{i,j}}{\sum_{k \neq j=1}^{m} 1/a_{k,j}}. \tag{15}$$

Since this probability is independent of R, when we allow R to go to infinity this number is not affected. It is thus natural to define a probability function P on L by

$$P(x \in L_{i,j}) = \frac{1/a_{i,j}}{\sum_{k \neq j=1}^{m} 1/a_{i,j}}. \tag{16}$$

It is easy to check that P is a probability function. It depends only on the areas of the parallelograms that are determined by the pairs of the given families of lines.

The three-dimensional generalization is now obvious. Families of parallel lines are replaced by families of parallel planes and parallelograms by parallelepipeds determined by three planes. If we are given m families $\Lambda_1, \ldots, \Lambda_m$ of parallel planes and want the probability that a given intersection point $x \in m$ belongs to the set

Fig. 4. The abandoned gypsum quarry at the Ramon crater, Israel.

L_{ijk} determined by $\Lambda_i \cap \Lambda_j \cap \Lambda_k$, then

$$P(x \in L_{i,j,k}) = \frac{1/V_{i,j,k}}{\sum_{l\neq r\neq s=1}^{m} 1/V_{l,r,s}} \quad (17)$$

where $V_{l,r,s}$ is the volume of the parallelepiped determined by members of the families Λ_l, Λ_r, Λ_s.

5. A rock engineering application

In this section an application of the concepts is presented using a real example from an abandoned gypsum quarry in Southern Israel. The north-west side wall of the quarry will be used as a free surface to demonstrate our approach (Fig. 4).

5.1. Rock mass characteristics

The rock mass at the quarry consists of a bedded and jointed gypsum sequence of the Triassic Mohila formation which consists primarily of gypsum, anhydrite, and some dolomite layers. The quarry was developed at the crest of the Ramon anticline where the Triassic sequence is exposed. The rock mass structure consists of three steeply inclined and very persistent joints sets (J_1, J_2, and J_3), and a set of bedding planes (J_4). The dip and dip direction, mean spacing, and friction angle of the joint sets are listed in Table 1 below. A joint trace generation for the analyzed free surface using actual orientation and spacing data is demonstrated in Fig. 5 using the joint generation code in DDA [16].

Table 1
Characterization of the principal joint sets in the abandoned gypsum quarry at the Ramon crater, Israel

Joint set #	Dip	Dip direction	Mean spacing (m)	Peak friction angle (°)
1	84	146	1.77	58
2	77	62	0.70	58
3	82	88	2.36	58
4 (bedding)	14	237	0.44	58

5.2. Block theory analysis

Consider the analyzed free surface which dips 90/115. By Section 2.1 the number of joints in any intersection cannot be greater than $k = 3$, and therefore $N = \binom{m}{k} = \binom{4}{3} = 4$. The joint intersections, removable JP codes, failure mode, factor of safety, and normalized support force (F^*/R) are listed in Table 2 below. Block theory removability analysis and the geometries of the removable blocks with respect to the analyzed free surface are illustrated in Fig. 1. An equal distance of 1 m from each boundary joint to the block center was used as input in the generation of the three-dimensional block geometries, i.e. the actual spacing values were overlooked. This simplification allows a comparative discussion of block shapes, rather than a specific discussion of block volumes that would have been possible if actual spacing values were used.

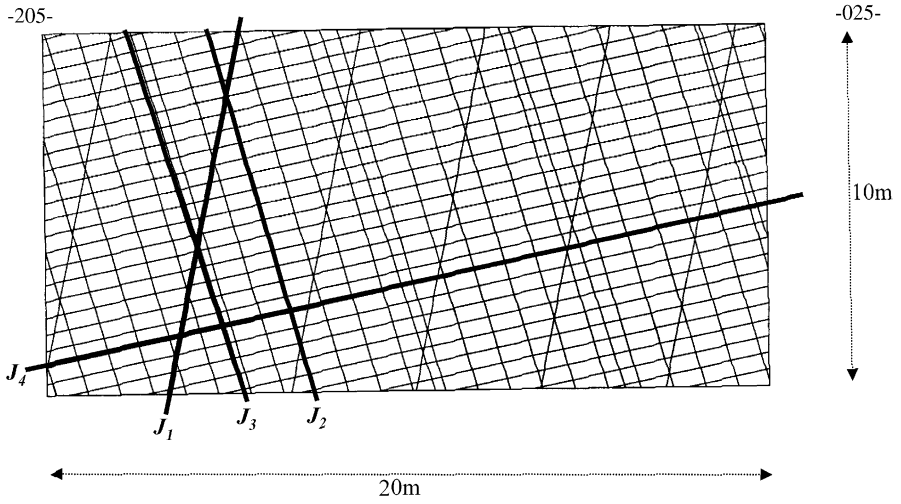

Fig. 5. Statistical joint trace generation using joint data in Table 1 as seen on the analyzed free surface.

Table 2
Results of block theory analysis

Joint intersection (L_{ijk})	*i,j,k*	Removable JP code	Failure mode	Factor of safety against sliding	Normalized support force
1	1,2,3	110	3	0.22	0.767
2	1,2,4	001	12	0.48	0.503
3	1,3,4	001	13	0.26	0.736
4	2,3,4	101	3	0.22	0.767

Free surface orientation: 90/115. Rock mass structure as in Table 1. In the JP code column upper and lower half spaces are denoted by 0 and 1 respectively. In the failure mode column modes *i* and *ij* indicate single or double plane sliding respectively. The factor of safety is calculated assuming equal friction angle for all joints. The normalized support force is the required support force for limit equilibrium normalized by the block weight.

By inspection of Fig. 1 it becomes immediately apparent that every joint intersection which contains the intersection $J_2 \cap J_3$ is *safe* because although $I_{2,3}$ plots inside the space pyramid it projects very close to the free surface (Figs. 1A and D). Joint intersections 1 and 4 are therefore *safe* and need not be analyzed any further.

5.3. Determination of the joint intersection probability

A mathematical expression for the joint intersection probability is given by Eq. (17) above. To apply Eq. (17) the volumes of the different types of parallelepipeds which result from all joint intersections $L_{i,j,k}$ must be determined.

The volume of a parallelepiped formed by the intersection of *i*, *j*, *k* in a coordinate system, where the *x* axis is horizontal pointing north, the *y* axis is horizontal pointing west, and the *z* axis is vertical pointing up, is given by (Fig. 6):

$$V_{i,j,k} = \overline{n}_i \bullet (\overline{n_j} \times \overline{n_k}) = \begin{vmatrix} x_i \cos\delta_i \cos\beta_i & x_i \cos\delta_i \sin\beta_i & x_i \sin\delta_i \\ x_j \cos\delta_i \cos\beta & x_j \cos\delta_i \sin\beta & x_j \sin\delta_i \\ x_k \cos\delta_i \cos\beta & x_k \cos\delta_i \sin\beta & x_k \sin\delta_i \end{vmatrix}, \quad (18)$$

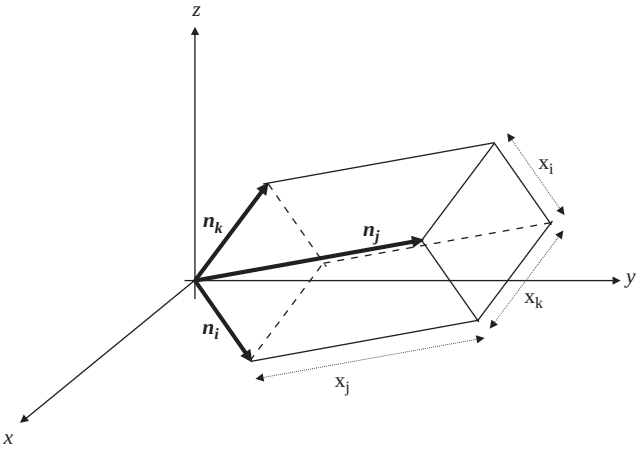

Fig. 6. The volume of a parallelepiped formed by intersections of joints *i,j,k*.

where n_i and x_i are the upward normal and mean spacing of joint set *i*, respectively. The direction cosines of the normal vector are given by δ_i and β_i, where δ_i is the rise angle of upward normal *i* with respect to plane *xy*, and β_i is the angle from the *x* axis to the trace of normal *i* on plane *xy* measured counterclockwise from *x*.

Table 3
The joint intersection probabilities for the analyzed free surface

$L_{i,j,k}$	i,j,k	$V_{i,j,k}$ m^3	$P_{i,j,k}$
1	1,2,3	0.286459	0.380921
2	1,2,4	0.538108	0.202781
3	1,3,4	1.527292	0.071445
4	2,3,4	0.316419	0.344853

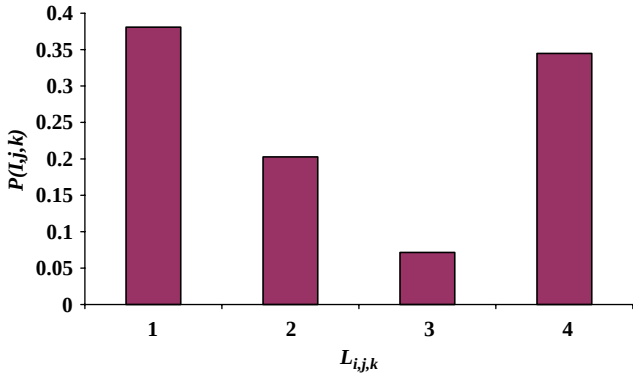

Fig. 7. The joint intersection probability computed for the analyzed free surface.

In Table 3 all the steps required for the computation of the joint intersection probability for the analyzed free surface are demonstrated and the results are plotted in Fig. 7.

5.4. The critical key block in the excavation

Inspection of Fig. 7 quickly reveals that $L_{ijk} = 1$, and 4 have the highest joint intersection probability. However, as explained above, these two joint intersections contain $I_{2,3}$ and are, therefore, designated *safe*. Indeed, a careful investigation of the rock slope in the field revealed no such blocks.

To determine which of the remaining JPs have the highest failure likelihood the stability of the two JPs must be considered. As shown in Table 2 the removable JPs from intersections $L_{ijk} = 2$, and 3 have the same JP code: 001, and the same failure mode: I_{ij}. In the case of joint intersection 2 failure is by sliding along $I_{1,2}$ and in the case of $L_{ijk} = 3$ failure is by sliding along $I_{1,3}$. Since $I_{1,3}$ is steeper than $I_{1,2}$ it is less stable and therefore the associated factor of safety for the removable JP of $L_{1,3,4}$ is lower. To account for block instability the original [11] instability parameter (F) must be employed:

$$F = 2^{((F^*/R)-1)}, \tag{19}$$

where F^* is the support force required for limit equilibrium and R is the block weight (the active resultant in a dry case).

Table 4
The block failure likelihood for the analyzed free surface (the critical key block row is shaded)

$L_{i,j,k}$	i,j,k	$P_{i,j,k}$	F	$P(B)$
1	1,2,3	0.380921	0.767	Safe Intersection
2	1,2,4	0.202781	0.503	0.143686305
3	1,3,4	0.071445	0.736	0.059498023
4	2,3,4	0.344853	0.767	Safe Intersection

The critical key block is found by finding the block failure likelihood ($P(B)$) for every joint combination after deleting the "safe" intersections:

$$P(B) = P(x \in L_{i,j,k})F. \tag{20}$$

The instability parameters and failure likelihoods for L_{ijk} 2 and 3 are listed in Table 4. From Table 4 it is evident that joint intersection 2 produces the critical key block in the analyzed excavation. Indeed, the majority of block moulds which were mapped in the field when the analyzed free face was surveyed belonged to L_{ijk} 2. Two typical examples are shown in Fig. 8 which shows characteristic block moulds of intersection 2, all of which exhibit a JP code of 001 and a failure mode of $I_{1,2}$.

6. Summary and conclusions

- It is proven in this paper that the probability of more than three joints (representative of three principal joint sets) passing through the same intersection in a jointed rock mass is zero.
- This result reduces significantly the outcome space of theoretically removable JPs in a jointed rock mass from an analyzed free surface and allows an efficient application of block theory.
- A rigorous expression for the joint intersection probability is developed in this paper. The joint intersection probability is given by

$$P(x \in L_{i,j,k}) = \frac{1/V_{i,j,k}}{\sum_{l\neq r\neq s=1}^{m} 1/V_{l,r,s}},$$

where $V_{i,j,k}$ is the volume of the parallelepiped formed by intersection $L_{i,j,k}$.

- The joint intersection probability is inversely proportional to the mean spacing of the joint sets which participate in the intersection. With increasing mean spacing the volume of the parallelepiped increases and therefore the joint intersection probability decreases.

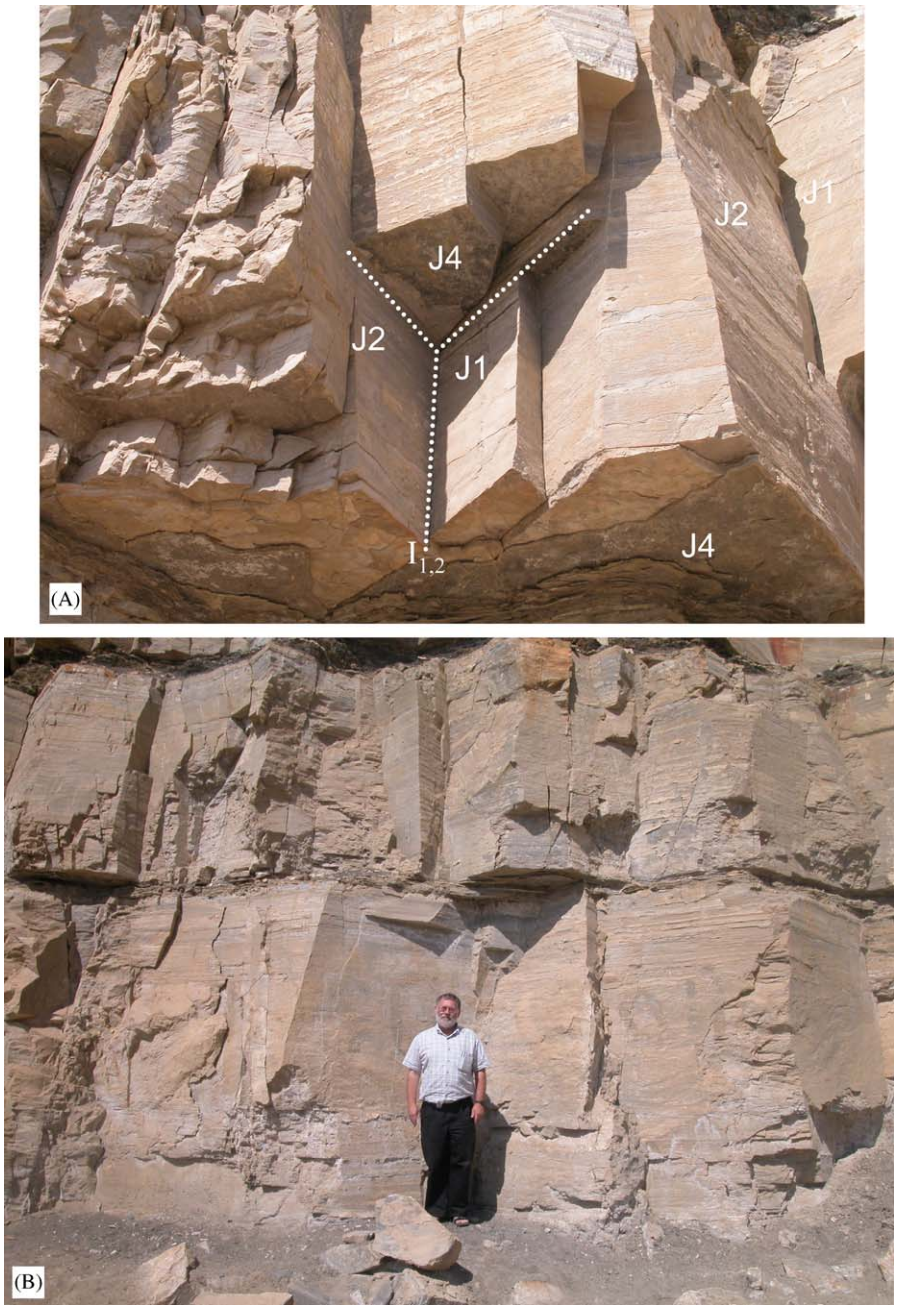

Fig. 8. The critical key block in the analyzed free surface. (A) A relatively small block mould of the critical key block, (B) a relatively large block mould of the critical key block.

- Two factors influence the block failure likelihood in the rock mass: (1) the joint intersection probability and (2) the instability of the associated key block. Therefore, the joint intersection probability must be conditioned by the block instability parameter to obtain a correct block failure likelihood.
- Joint intersections may be safe and incapable of producing removable key blocks when a line of intersection I_{ij} in the joint intersection L_{ijk} is parallel or even sub-parallel to the analyzed free surface. Such joint intersections may be excluded from further analysis.

Acknowledgement

The students of the Rock Slope Engineering course of spring 2004 at BGU are thanked for providing the structural data which were used in the example.

References

[1] Goodman RE. Methods of geological engineering in discontinuous rocks. St. Paul: West Publishing Company; 1976.

[2] Priest SD. Hemispherical projection methods in rock mechanics. London: George Allen & Unwin; 1985.
[3] Priest SD, Hudson JA. Discontinuity spacing in rock. Int J Rock Mech Min Sci & Geomech Abstr 1976;17:1–23.
[4] Priest SD, Hudson JA. Estimation of discontinuity spacing and trace length using scanline surveys. Int J Rock Mech Min Sci & Geomech Abstr 1981;18:183–97.
[5] Mauldon M. Estimating mean fracture trace length and density from observations in convex windows. Rock Mech Rock Eng 1998;31(4):201–16.
[6] Zhang L, Einstein HH. Estimating the mean trace length of rock discontinuities. Rock Mech Rock Eng 1998;31: 217–34.
[7] Goodman RE, Shi G-H. Block theory and its application to rock engineering. Englewood Cliffs, NJ: Prentice-Hall; 1985.
[8] Londe PF, Vigier G, Vormeringer R. Stability of rock slopes—graphical methods. J Soil Mech Foundns Div ASCE 1970;96(SM4):1411–34.
[9] Hatzor Y. Validation of block theory using field case histories. PhD thesis. Department of Civil Engineering, University of California, Berkeley, 1992.
[10] Hatzor Y, Goodman RE. Application of block theory and the critical key block concept to tunneling: two case histories. In: Myer LR, Cook NGW, Goodman RE, Tsang C, editors. Proceedings of ISRM conference on fractured and jointed rock masses. Balkema: Rotterdam; 1992. p. 663–70.
[11] Hatzor Y. The block failure likelihood: A contribution to rock engineering in blocky rock masses. Int J Rock Mech Min Sci 1993;30(7):1591–7.
[12] Hatzor YH, Goodman RE. Three-dimensional back analysis of saturated rock slopes in discontinuous rock—a case study. Geotechnique 1997;47(4):817–39.
[13] Mauldon M. Relative probabilities of joint intersections. In: Tillerson, Wawersik, editors. Rock Mechanics. Proceedings of the 33rd U.S. Rock Mechanics, Symposium. Santa Fe, New Mexico: Balkema, Rotterdam; 1992. p. 767–74.
[14] Fisher R. Dispersion on a sphere. Proc Roy Soc 1953;A217:295–305.
[15] Dwass M. Probability theory and applications. New York: Benjamin; 1970.
[16] Shi G-H. Block system modeling by discontinuous deformation analysis. Southampton UK: Computational Mechanics Publications; 1993. p. 209.